

Excitability and coherence resonance in lasers with saturable absorber

Johan L. A. Dubbeldam,^{1,*} Bernd Krauskopf,² and Daan Lenstra¹

¹*Faculty of Sciences, Vrije Universiteit, De Boelelaan 1081, 1081 HV Amsterdam, The Netherlands*

²*Department of Engineering Mathematics, University of Bristol, Bristol BS8 1TR, United Kingdom*

(Received 15 July 1999)

We show that a laser with a saturable absorber, described by the Yamada model, displays excitability just below threshold. A small perturbation, for example, a small input pulse, can trigger a single high output pulse, after which the system relaxes back to the off state. In order to study possible applications, such as pulse reshaping and clock recovery, approximate expressions are given for the excitability threshold and the delay between input and output pulses. Under the influence of optical noise, the system displays coherence resonance: below threshold the laser produces pulse trains with minimal jitter for a particular optimal noise level. This all-optical coherence resonance allows direct experimental verification.

[S1063-651X(99)02712-9]

PACS number(s): 05.45.-a, 42.55.Px

I. INTRODUCTION

The notion of excitability comes from biology and chemistry where excitable systems have been known for some time now [1]. Spreading excitation waves were observed in a great variety of reaction diffusion systems, such as cardiac muscle tissue and the Belousov-Zhabotinsky reaction [2]. Excitability is also an important concept in neuronal modeling, where it is considered to constitute the mechanism behind the spiking behavior of nerve cells [1,3]. More recently, excitability has also been found in optical systems, namely in nonlinear cavities with temperature-dependent absorption [4], lasers with optical feedback, [5] and lasers with a saturable absorber [6].

Following the biology literature [1,7], a system is said to be *excitable* if it is at an attracting equilibrium state, but can be triggered by a sufficiently large but still small perturbation to produce a large amplitude excursion, after which the system settles back to the attractor in what is called the *refractory phase*. After the refractory phase, the system can be triggered again. There are essentially two known types of excitability. First, there is excitability due to an S-shaped slow manifold in slow-fast systems as in the FitzHugh-Nagumo model of neuron spiking [1,3,7] as sketched in Fig. 1(a). A (sufficiently large) perturbation can bring the system from the attractor to the white dot in the phase portrait on the left. From there the system makes a quick jump to the right branch of the slow manifold, which it then traces before it jumps back to the left branch and relaxes back to the attractor. This leads to a square-shaped pulse as sketched on the right of Fig. 1(a). Second, there is excitability due to an attractor close to a saddle point on an attracting invariant circle [8,9] as sketched on the left in Fig. 1(b). The fact that the attractor and the saddle point are close together means that the system is close to a saddle-node bifurcation on a limit cycle (also called infinite period saddle-node bifurcation or codimension-1 homoclinic saddle-node bifurcation).

A perturbation moving the system across the saddle point to the white dot results in a large amplitude excursion around the invariant circle. This corresponds to a single pulse as sketched on the right side of Fig. 1(b). There may be several pairs of attractors and saddle points on the invariant circle with the possibility of multistability [10]. Note that in both types of excitability the amplitude of the excursion is independent of the perturbation, because the slow manifold and the invariant circle determine the maximum of the pulse, respectively.

In this paper, we study excitability in a semiconductor laser with a saturable absorber modeled by the Yamada model [11]. This system, which is of a slow-fast nature, constitutes a simple model for Q switching in semiconductor lasers. Its dynamics and bifurcations were recently studied in much detail in Ref. [6], where it was noted that the system is excitable just before threshold. Here we study this type of excitability and the dynamical consequences thereof. The

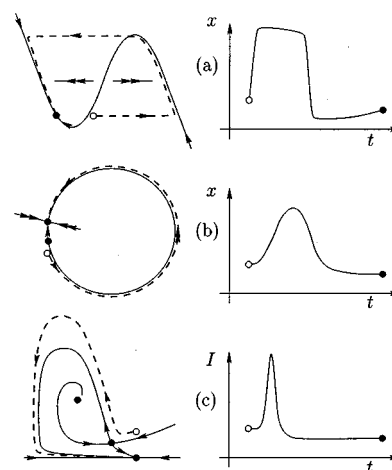


FIG. 1. Three types of excitable systems sketched as phase portraits (left column), together with the respective time series of the response to a perturbation (right column): the classical S-shaped slow manifold as in the FitzHugh-Nagumo equation (a), an attractor close to a saddle point on an attracting invariant circle (b), and the excitability of a laser with absorber studied here.

*Author to whom correspondence should be addressed. FAX: +31-20-444-7899. Electronic address: dubbeldm@nat.vu.nl

situation is sketched in Fig. 1(c) and can be explained as follows. The off solution with $I=0$ is an attractor, but a perturbation can push the system above the stable manifold to the white dot in the phase portrait on the left. From there the system produces a single intensity pulse and then relaxes slowly back to the off solution by creeping along the slow manifold $\{I=0\}$. The pulse is very short compared to the refractory phase, as is sketched on the right side of Fig. 1(c). In the Yamada model there is no upper limit to the height of a pulse, which turns out to depend linearly on the energy of the input pulse; see later sections for more details. Since self-pulsations have been found in semiconductor lasers both in the stripe [11–13] and the longitudinal configuration [14], we expect this excitability to be detectable experimentally.

Excitability in this laser has a number of potential applications. The laser could be used as an optical switch, which reacts only to sufficiently high optical input signals. This could be used for clock recovery. The main application we investigate here is pulse reshaping: a small wide input pulse can trigger a large short output pulse. We numerically investigate this and show that the shape of the output pulse is independent of the shape of the input pulse. The pulse height depends on the energy of the input pulse, but also on the parameter values, and in particular on the gain and absorber relaxation rate γ [15]. By exploiting the slow-fast nature of the system, we derive analytical expressions for the *excitability threshold*, the minimal perturbation needed to trigger the system, and for the delay between input and output pulses. Finally, we show that spontaneous emission does not excite the system when operated sufficiently far below threshold, so that pulse reshaping appears to be possible in a realistic, noisy setting.

An effect closely related to excitability, and with potential applications for jitter reduction of pulse trains, is *coherence resonance* (CR). Below threshold the laser produces noise-induced pulse trains, and CR is the effect that their coherence is maximal for a particular noise level. Coherence resonance (in some sense a special case of stochastic resonance (SR) [16–19]) has recently been studied in a number of systems. In Ref. [10] it is shown that a two-dimensional dynamical system with an invariant circle [much like in Fig. 1(b)] can show CR. In the FitzHugh-Nagumo system [20] and in the Hodgkin-Huxley neuron model [21], CR due to excitability of type (a) in Fig. 1 has been found. Recently, CR has been reported experimentally in a semiconductor laser with optical feedback and noise in the pump source, which is probably due to excitability of type (b) in Fig. 1 [9].

Here we show that a laser with a saturable absorber displays all optical CR. This is a consequence of the excitability of type (c) in Fig. 1, and we expect CR to be observable experimentally. When optical noise is injected into the laser below threshold, the system produces a train of pulses. There is a minimum of the jitter of this pulse train, which is clear evidence that the system displays CR. There may very well be future applications of this effect for generating coherent pulse trains, for example for optical communication systems.

We proceed as follows. In Sec. II, the Yamada system is introduced and its basic dynamics and bifurcations are discussed as needed here. In Sec. III, excitability below threshold is discussed together with its use for pulse reshaping. In Sec. IV, we first study the influence of spontaneous-emission

noise and then we show that the system displays coherence resonance when optical noise is injected. We finally draw conclusions in Sec. V.

II. DYNAMICS OF THE YAMADA MODEL

The starting point of our analysis is the Yamada model without noise. This three-dimensional dynamical system is governed by the dimensionless equations

$$\begin{aligned}\dot{G} &= \gamma(A - G - GI), \\ \dot{Q} &= \gamma(B - Q - aQI), \\ \dot{I} &= (G - Q - 1)I,\end{aligned}\tag{1}$$

where G models the gain, Q the absorption, and I is the laser intensity. The parameters in Eqs. (1) have the following meaning: A is the bias current of the gain, B is the amount of absorption, and a describes the differential absorption relative to the differential gain. The parameter γ describes the relaxation rate of the gain and the absorber and it is small, typically of the order of 10^{-3} . The Yamada model is therefore a slow-fast system, where G and Q are the slow variables and I is the fast variable. The plane $\{I=0\}$ is invariant under the flow and at the same time a slow manifold of the system. This model is valid for two types of lasers with absorber: the two-segment laser and the stripe laser. For the two-segment laser, in which the gain and the absorber are spatially separated in the longitudinal direction, the decay times in the gain and the absorber need to be of the same order. For the stripe laser, in which the absorber is constituted by the unpumped regions accompanying the gain region on both sides in the transversal direction, the diffusion between the gain and the absorber needs to be negligible. Self-pulsating lasers of either type satisfying these assumptions are readily available.

The complete dynamics of Eqs. (1) was obtained in Ref. [6]. Here we concentrate on the parameter regime for which the system shows excitability. This is why we fix the absorption parameters to realistic values for a Q -switched laser. We choose $B=5.8$ and $a=1.8$ for the remainder of this paper, but any values of B and a would do as long as $B(a-1) > 1$. The exact value of γ is then not important, and for any $\gamma < 0.05$ the behavior of the laser is qualitatively as sketched in Fig. 2.

In the bifurcation diagram in the (A, I) plane as presented in Fig. 2, we plot in boldface the maximum of the intensity I versus the pump current A for the fixed value of $\gamma=0.04$. The dashed curve corresponds to unstable behavior as explained below. There are three bifurcations S , T , and H dividing the A line into four regions, denoted by 1 through 4, of different dynamics as presented by the four sketches of phase portraits. Note that the missing direction is always attracting, so that two-dimensional phase portraits suffice [6]. In Fig. 2 we plot the gain G horizontally and the intensity I vertically; the slow manifold $\{I=0\}$ is at the bottom of each phase portrait. In region 1 the only attractor is the off solution, the attractor on $\{I=0\}$. In the saddle-node bifurcations two saddle points are born, so that the phase portrait in region 2 still has the off solution as the only attractor. In the

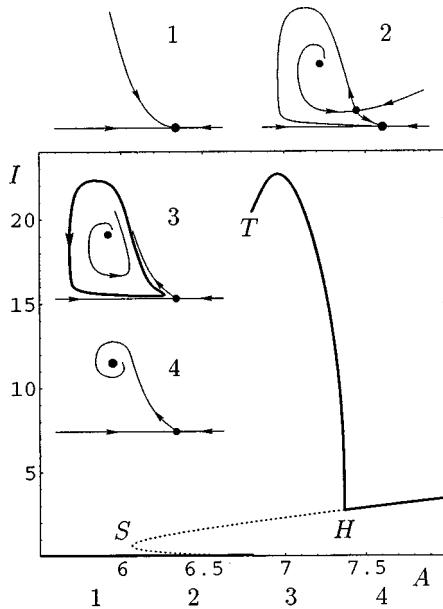


FIG. 2. The dynamics of a laser with absorber. The bifurcation diagram in the (A, I) plane features the three bifurcations S , T , and H , which divide the A axis into four regions of qualitatively different phase portraits as sketched. (Attractors are boldfaced.)

absence of an external perturbation, the laser is off. However, a single small perturbation can bring I above the stable manifold of the lower saddle point. This results in a single pulse in I , after which the laser settles back to the off solution; compare Fig. 1(c). In other words, the laser is excitable in region 2 for pump currents between S and T . The amplitude of the perturbation needed to create a pulse decreases as A is increased: the system is “most excitable” just before the threshold T . At T there is a homoclinic bifurcation practically simultaneous with a transcritical bifurcation [6]. As a consequence, a stable limit cycle appears and the lower saddle point vanishes, which physically means that the laser self-pulsates in region 3. The pulsations finally increase in frequency and become more sinusoidal before disappearing in the Hopf bifurcation H . In region 4 there is a single attractor with positive intensity, which corresponds to cw output of the laser.

III. EXCITABILITY

The laser with a saturable absorber is excitable before threshold in region 2 when its phase portrait is as sketched in the respective panel of Fig. 2. We now study this type of excitability in more detail. First, we consider the reaction of the laser to different input pulses. Second, we derive approximate expressions for the excitability threshold and the delay between incoming and outgoing pulses, which shows that the laser becomes indeed “more excitable” the closer to threshold it is operated.

A. Pulse reshaping

To find the exact influence of perturbations introduced into the system, we perform numerical simulations of Eqs. (1) for the fixed value of $A = 6.5$ (just before threshold) and for $\gamma = 0.001$. (Recall that we set $B = 5.8$ and $a = 1.8$.) Three

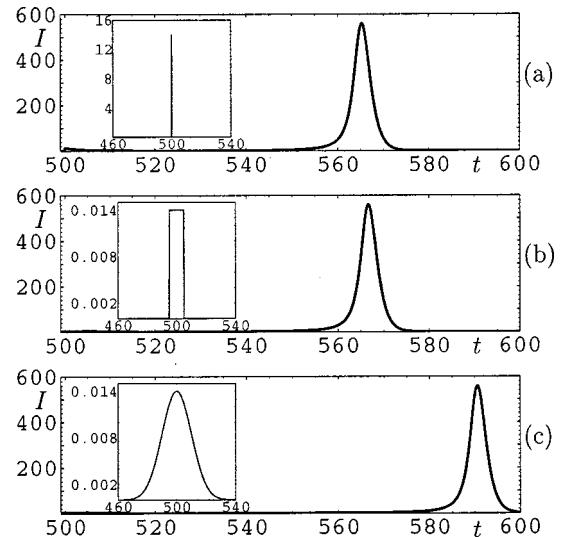


FIG. 3. Three different input pulses and the resulting output pulses for $A = 6.5$, $\gamma = 0.001$, $B = 5.8$, $a = 1.8$. The perturbation amplitude I_0 is 14 for the δ pulse and 0.014 for the block and Gaussian pulse.

different (triggering) input pulses were introduced into the system: a δ pulse, a block pulse, and a Gaussian pulse. In Fig. 3 we present the three output pulses for the three different triggering pulses. In Fig. 3(a) the input pulse is very short (δ peak signal), leading to a large output pulse. In Fig. 3(b) the input pulse is a block pulse of the same energy as the δ pulse. The resulting output pulse is practically equal to that for the δ input pulse. Moreover, the delay between the input pulse and the output pulse is equal for both cases. Finally, in Fig. 3(c) the input is a Gaussian pulse. The energy contained in the Gaussian pulse is a little greater than for the perturbations (a) and (b). This is necessary because, due to its more global nature, part of its energy is lost before it can contribute to triggering. Figure 3(c) shows that the produced output pulse has the same shape as before in panels (a) and (b), although it appears after a somewhat longer time. This indicates that the system is perturbed to a point closer to the stable manifold, which forms the excitability threshold.

The fact that for a perturbation with long tails, such as the Gaussian pulse, more energy is required to reach the excitability threshold, can be explained as follows. The energy contained in the tails is in some sense lost, because the intensity rise in the system due to the added intensity from the tails is canceled by the intensity decrease due to the system’s relaxation towards the stable equilibrium or “off-state” with coordinates $(G, Q, I) = (A, B, 0)$. Physically this means that the tails of a perturbation should be short with respect to the relaxation time of the gain and absorber, because otherwise relaxation will be the dominant process in the perturbation tails.

The discussion above illustrates that the delay between the incoming and outgoing pulses, defined as the time difference between the produced output peak and the input pulse maxima, is an important quantity. We numerically obtained the delay for different values of the perturbation amplitude I_0 of a Gaussian input pulse. In Fig. 4(a) the delay is depicted as a function of I_0 . It goes to infinity when the excitability threshold is approached and is a decreasing func-

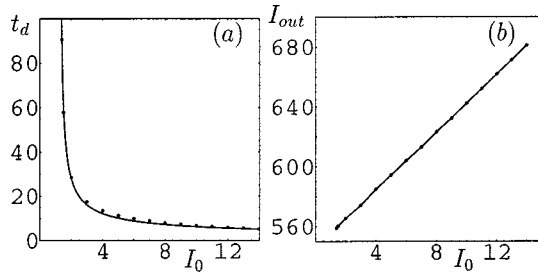


FIG. 4. The delay (a) between a Gaussian input pulse and the output pulse as a function of the amplitude I_0 . The dots denote the numerical results and the solid curve represents the analytical expression for t_d of Eq. (13) for $I_0^{\text{th}} = 1.3$. The output pulse amplitude (b) depends linearly on the perturbation amplitude relative to the excitability threshold.

tion of I_0 . The amplitude of the output pulse was also obtained by numerical simulation and is displayed in Fig. 4(b). As was mentioned before, the amplitude of the output pulse is not constant, but depends linearly on the amplitude of the input pulse relative to the excitability threshold. This can be understood as follows. All incoming pulses with sufficiently large amplitudes to trigger the system will experience the same net gain. Due to the slow evolution of the absorber and the gain, they only saturate after the output pulse attained its maximum, since here γGI and $a\gamma QI$ are of order 1. Clearly, there will not be a linear dependence of the output amplitude on the triggering pulse for very large triggering pulses due to the saturation effects, but we still expect that this linear dependence can be observed experimentally for sufficiently small input pulses.

B. Excitability threshold and delay

In this rather technical section, we concentrate on finding analytical expressions for the excitability threshold and the delay between incoming and outgoing pulses. Geometrically, the excitability threshold is determined by the distance between the attractor and the stable manifold of the saddle point; see Fig. 1(c). To derive an analytical expression of the excitability threshold, we make use of the slow-fast nature of the system, meaning that the gain and the absorber evolve on a much longer time scale than the intensity. The method of multiple scales [22] from singular perturbation theory was used in Ref. [15] to obtain an asymptotic expression for the period of the pulsations for a laser operating very close to the lasing threshold. However, in our present setting the system is perturbed by an order 1 perturbation (the excitability threshold is of order 1), as can be seen from the numerical computations in Fig. 5. This is why we use a different method, which, however, also uses the slow-fast nature of the system.

We assume that the system is initially at the equilibrium state $(G, Q, I) = (A, B, 0)$ and that at $t=0$ a δ shaped triggering signal $I_{\text{pert}} = I_0 \delta(t)$ is applied to the system. The assumption of a δ pulse can be relaxed and it is sufficient that the incoming pulse is of a much shorter duration than the relaxation time of the gain and the absorber. Because of the slow evolution of the gain and the absorber, we can solve Eqs. (1) for G and Q in the first-order approximation in δG and δQ by substituting

$$G = A + \delta G, \quad Q = B + \delta Q$$

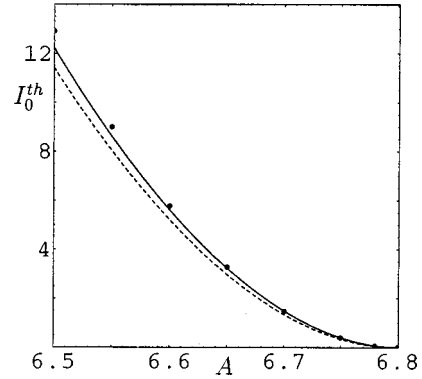


FIG. 5. The excitability threshold as a function of the pump parameter A . The dots denote numerical data, the dashed curve is the first-order approximation I_1^{th} of Eq. (10), and the solid curve is the second-order approximation I_2^{th} of Eq. (12).

into Eqs. (1), which leads to the following expressions for the gain and the absorber:

$$G = A - \gamma A \left[\int_0^t e^{\gamma t'} I(t') dt' \right] e^{-\gamma t},$$

$$Q = B - \gamma a B \left[\int_0^t e^{\gamma t'} I(t') dt' \right] e^{-\gamma t}.$$
(2)

These expressions are only valid when G differs only a little from A , and Q only a little from B . Substituting Eqs. (2) into Eqs. (1) gives after differentiation the second-order differential equation for the intensity,

$$\ddot{I} - \dot{I}^2 + \gamma I \dot{I} = \gamma [(A - B - 1) + (aB - A)I] I^2. \quad (3)$$

The initial conditions of Eq. (3) are $I(0) = I_0$, which implies that $\dot{I}(0) = (A - B - 1)I_0$. Introducing rescaled variables $y(t) = I(t)/I_0$ and defining $\alpha = B + 1 - A$, we can rewrite Eq. (3) in the more suitable form

$$\ddot{y} y - \dot{y}^2 + \gamma y \dot{y} = -\gamma \alpha y^2 + \gamma (aB - A) I_0 y^3,$$

$$y(0) = 1, \quad \dot{y}(0) = -\alpha. \quad (4)$$

All terms linear in γ except the y^3 term on the right-hand side of Eq. (4) are small, so Eq. (4) is reduced to

$$\ddot{y} y - \dot{y}^2 = \gamma (aB - A) I_0 y^3, \quad y(0) = 1, \quad \dot{y}(0) = -\alpha, \quad (5)$$

which can be solved exactly by assuming a solution of the form

$$\dot{y} = f(y). \quad (6)$$

From the initial conditions on y it follows that $f(1) = -\alpha$. Substituting the expression for \dot{y} into Eq. (4), we obtain

$$(f^2)' - \frac{2f^2}{y} = 2\gamma (aB - A) I_0 y^2, \quad (7)$$

where the prime indicates differentiation with respect to y . Equation (7) can be solved as

$$f(y) = -\sqrt{\alpha^2 - 2\gamma(aB-A)I_0 + 2\gamma(aB-A)I_0y} y. \quad (8)$$

From Eq. (8), $y(t)$ can be obtained by integration as

$$y(t) = \frac{\beta^2 - \alpha^2}{\beta^2} \left[1 + \tan^2 \left(\phi_0 - \frac{\sqrt{\beta^2 - \alpha^2}}{2} t \right) \right], \quad (9)$$

where we introduced β^2 and ϕ_0 defined by

$$\beta^2 = 2\gamma I_0(aB-A), \quad \phi_0 = \arctan \left(\frac{\alpha}{\sqrt{\beta^2 - \alpha^2}} \right).$$

The minimal perturbation amplitude necessary to trigger the system, or to bring the system above the stable manifold of the saddle, is determined by the requirement of the existence of a nontrivial (positive y) solution of $\dot{y}=0$. In terms of gain and absorption this means that there must be some instance for which the gain exceeds the total loss, which means that the plane $\{G-Q-1=0\}$ must be crossed. Such a solution is only possible if the y -independent term under the square root in Eq. (8) is less than zero. The excitability threshold is therefore the value of I_0 for which this term vanishes. This gives the first-order approximation for the excitability threshold,

$$I_1^{\text{th}} = \frac{\alpha^2}{2\gamma(aB-A)} = \frac{(B+1-A)^2}{2\gamma(aB-A)}. \quad (10)$$

This expression can be improved by realizing that the largest error comes from the first-order approximation of gain and absorption in Eq. (2). Using Eq. (9), one obtains the second-order approximation for G and Q ,

$$\begin{aligned} G &= A - \frac{\gamma A e^{-\gamma t}}{aB-A} \left[(aB-B-1) \int_0^t e^{\gamma t'} I(t') dt' \right. \\ &\quad \left. + \int_0^t \sqrt{\alpha^2 - \beta^2 + \beta^2 y} I(t') e^{\gamma t'} dt' \right], \\ Q &= B - \frac{\gamma aB e^{-\gamma t}}{aB-A} \left[(aB-B-1) \int_0^t e^{\gamma t'} I(t') dt' \right. \\ &\quad \left. + \int_0^t \sqrt{\alpha^2 - \beta^2 + \beta^2 y} I(t') e^{\gamma t'} dt' \right]. \end{aligned}$$

The differential equation (4) in the second order approximation becomes

$$\ddot{y} - \dot{y}^2 + \gamma y \dot{y} = -\gamma \alpha y^2 + \gamma I_0 y^3 (aB-B-1) + \gamma I_0 \sqrt{\beta^2 y + \alpha^2 - \beta^2} y^3 \quad (11)$$

with the same initial condition as in Eq. (4). Solving Eq. (11) in the same way as Eq. (4) gives a second-order approximation of the excitability threshold,

$$\begin{aligned} I_2^{\text{th}} &= \frac{\alpha^2}{2\gamma(aB-B-1)} \left(1 - \frac{2\alpha}{3(aB-A)} \right) \\ &\quad + \frac{\alpha}{aB-B-1} \left[1 - \ln \left(\frac{2\gamma}{\alpha} \right) \right], \quad (12) \end{aligned}$$

where the last term on the right-hand-side is due to the $\gamma y \dot{y}$ and $\gamma \alpha y^2$ terms.

In Fig. 5 these two expressions for the excitability threshold are compared with the excitability threshold obtained numerically. This demonstrates that Eq. (10) is a fairly good approximation to within 10%, and the second-order approximation given by Eq. (12) is accurate to within 5%.

A first-order approximation of the delay between incoming and outgoing pulses can be obtained as follows. When the system is above threshold, the time at which \dot{y} changes sign, which we call t_d , can be found by integrating Eq. (6) or using Eq. (9), which gives

$$t_d = \frac{2}{\sqrt{\left(1 - \frac{I_0^{\text{th}}}{I_0}\right) [2\gamma(aB-A)I_0]}} \arctan \left(\frac{1}{\sqrt{\left(1 - \frac{I_0^{\text{th}}}{I_0}\right)}} \right). \quad (13)$$

This time t_d constitutes the dominant contribution to the delay, because the contribution of the output pulse duration to the delay is usually much smaller and can therefore be neglected. In Fig. 4(a), the numerically obtained values for the delay of a Gaussian triggering pulse are compared with the delay time t_d given by Eq. (13), into which we substituted the numerically obtained value for the threshold intensity I_0^{th} . Notice the good agreement between the two.

IV. THE EFFECT OF NOISE

Here we consider the effect of spontaneous emission and injection noise in the excitability regime and ultimately use injection noise to trigger the system and obtain a series of pulses. In order to study spontaneous-emission noise and indicate how noise terms enter the evolution equations, we start from the nonscaled equations

$$\begin{aligned} \dot{N}_1 &= J_p - \frac{N_1}{\tau_s} - g_1(N_1 - N_{t1})S, \\ \dot{N}_2 &= -\frac{N_2}{\tau_s} - g_2(N_2 - N_{t2})S, \quad (14) \end{aligned}$$

$$\dot{S} = [g_1(N_1 - N_{t1}) + g_2(N_2 - N_{t2}) - \Gamma_0]S + R_{\text{sp}} + F_s(t).$$

Here the number of electron-hole pairs in the pumped region is denoted by N_1 , the number of electron-hole pairs in the unpumped region by N_2 , and the number of photons by S . Further, J_p is the pump current and Γ_0 is the inverse photon lifetime. The transparency values for the gain and the absorber are N_{t1} and N_{t2} , respectively. The carrier lifetime is τ_s and the differential gain in region one is given by g_1 , while g_2 denotes the differential absorption in region two. The dimensionless pump parameter A is related to the bias pump current J_p by

$$A = \frac{g_1 \tau_s}{\Gamma_0} \left(J_p - \frac{N_{t1}}{\tau_s} \right).$$

The noise terms R_{sp} and $F_s(t)$ are as in Ref. [13] given by

$$R_{\text{sp}} = \frac{\beta N_1}{\tau_s}, \quad \langle F_{\text{sp}}(t_1) F_{\text{sp}}(t_2) \rangle = 2R_{\text{sp}} S \delta(t_1 - t_2).$$

By performing a transformation as in Ref. [6] and by adding a term $K_{\text{inj}}(t)$ for injected optical noise, Eqs. (14) are transformed into

$$\begin{aligned} \dot{G} &= \gamma(A - G - GI), \\ \dot{Q} &= \gamma(B - Q - aQI), \end{aligned} \quad (15)$$

$$\dot{I} = (G - Q - 1)I + \beta_{\text{sp}}(G + P) + D + K_{\text{sp}}(t) + K_{\text{inj}}(t).$$

The stochastic term representing the Gaussian spontaneous emission satisfies

$$\langle K_{\text{sp}}(t_1) K_{\text{sp}}(t_2) \rangle = 2\beta_{\text{sp}}(G + P)I \delta(t_1 - t_2), \quad \langle K_{\text{sp}}(t) \rangle = 0.$$

Furthermore, P is a constant term (transparency offset or gain) given by $P = N_{t1} g_1 / \Gamma_0$, which is numerically equal to 2.466 in our simulations. The spontaneous emission noise strength as given by the β_{sp} factor is typically of the order of 10^{-5} for semiconductor lasers [13]. Finally, $K_{\text{inj}}(t)$ is optically injected Gaussian noise satisfying

$$\langle K_{\text{inj}}(t_1) K_{\text{inj}}(t_2) \rangle = 2DI \delta(t_1 - t_2), \quad \langle K_{\text{inj}}(t) \rangle = 0.$$

Here D denotes the strength of the injection noise. The system with only injection noise is equivalent to the system as described in Ref. [23].

In all numerical simulations we take $a = 1.8$, $B = 5.8$, $A = 6.5$, and $\gamma = 0.001$, corresponding to the following values of the nonscaled variables [12]: $N_{t1} = 6.72 \times 10^7$, $N_{t2} = 9.0 \times 10^7$, $\tau_s = 3.0$ ns and $g_1 = 1.435 \times 10^{-8}$ ps $^{-1}$, $g_2 = 2.252 \times 10^{-8}$ ps $^{-1}$, and finally $\Gamma_0 = 0.3$ ps $^{-1}$ and $J_p = 13.0$ mA.

We remark that numerical simulations show qualitatively the same effects independent of the realization of the noise. This demonstrates an insensitivity of the model to the particular implementation of noise.

A. Spontaneous-emission noise and the noise threshold

In order to study the influence of spontaneous-emission noise, we set D equal to zero in Eq. (15). To find its effect on the output pulse shape and the excitability threshold, we performed numerical simulations of Eqs. (15) for several values of the spontaneous-emission factor β_{sp} . We found that spontaneous-emission noise does not lead to significant changes in the excitability threshold and the amplitude of the outgoing pulse. This can also be illustrated by the following argument. If one considers once more the phase portrait of Fig. 2 in the excitability regime 2, it can be seen that the noise needs to be at least strong enough to bring the intensity above the stable manifold at the lowest possible barrier. This barrier is given by the position of the saddle point, which lies in the $\{G - Q - 1 = 0\}$ plane and has the I value

$$I_{\text{sp}} = \frac{-B - 1 - a + aA}{2a} - \frac{\sqrt{(B + 1 + a - aA)^2 - 4(1 + B - A)a}}{2a},$$

which is numerically equal to 0.102 for our parameter values. The value of I_{sp} can be considered as the value of the noise threshold. If Eq. (15) is transformed into a Fokker-Plank equation [24,25], the Kramers escape time from the point $(G, Q, I) = (A, B, 0)$ to (A, B, I_{sp}) can be calculated as

$$T_{\text{esc}} = \frac{1}{D} \int_0^{\sqrt{I_{\text{sp}}}} dx e^{0.3x^2/D} \int_0^x dy e^{-0.3y^2/D}. \quad (16)$$

Numerically this gives $T_{\text{esc}} \approx 10^{1324}$ for $D = 10^{-5}$, which shows that spontaneous emission by itself is not capable of exciting the system. (For comparison, note that $T_{\text{esc}} \approx 20$ for $D = 0.01$.) One should notice that the values of I_{sp} and T_{esc} depend on the parameters and particularly on the pump current. Very close to threshold ($A \rightarrow T$), I_{sp} and T_{esc} become practically zero. This means that sufficiently close to the threshold T , spontaneous emission can excite the system and produce a sequence of pulses. However, here we are interested in values of A sufficiently far below the threshold T , where spontaneous emission cannot trigger the system. We conclude that for ordinary values of β_{sp} , the excitable laser below threshold can be used for pulse reshaping and noise filtering.

An interesting topic for future research is the idea of self-triggering a laser with a saturable absorber in the excitability regime. When a part of each produced output pulse is fed back into the laser after an excursion through a fiber, this is expected to produce very regular output pulses, whose frequency is tunable by changing the length of the fiber. Note that this is different from self-seeded gain switched lasers [26], because the pump current is constant and the pulses are produced by Q switching.

B. Coherence resonance

In the region of excitability, we numerically simulated Eqs. (15) (with noise) by a simple forward Euler algorithm and averaged over at least 2000 cycles. Throughout all simulations, we fixed $B = 5.8$, $a = 1.8$, and $\gamma = 0.001$; the spontaneous emission was set to $\beta_{\text{sp}} = 1.0 \times 10^{-5}$ and the pump current was $A = 6.50$, which is well in the excitability region [6.06,6.8]. We then considered the influence of injected noise of variable level D .

The injected noise, being much larger than spontaneous-emission noise, triggers the laser to produce pulse trains; three examples are shown in Fig. 6 for three different noise levels D . Coherence resonance manifests itself as an increased coherence of the pulse train for a particular noise level. It is known that small pump noise in combination with a periodic driving of the pump current can produce SR in lasers with a saturable absorber [27]. Furthermore, CR due to the addition of noise in the pump current has recently been found in a laser with optical feedback [9]. However, in the present setting adding noise to the pump current is not an efficient way of producing CR. Highly irregular pulses are obtained and an unrealistically high noise level (of the order of the dc pump current) is needed to produce an effect. This is why we study all optical CR.

The pulse train in Fig. 6(b) for $D = 0.015$ is most coherent. This effect of CR is not easy to see from the time series, but is evidenced by the corresponding power spectra

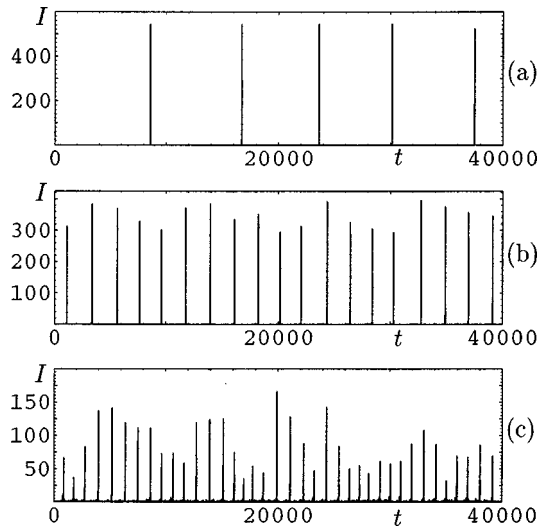


FIG. 6. Time series of $I(t)$ for a laser with fixed spontaneous emission of $\beta_{sp}=1.0\times 10^{-5}$ and for three different values of the injected noise level show CR. For $D=0.004 < D^R$ (a) the average pulse repetition time is 6837, for $D=0.015 = D^R$ (b) it is 2063, and for $D=0.04 > D^R$ (c) it is 1014.

$\langle S(\nu) \rangle = \langle |I(\nu)|^2 \rangle$ in Fig. 7, which were obtained by averaging over 100 different time series $[I(t)]$. The signal-to-noise ratio (SNR) of the spectrum is defined as $H_p / (\Delta\omega / \omega_p)$ and can be used as a quantitative measure for CR. Here, H_p is the relative height of the (first harmonic) peak in the spectrum and $(\Delta\omega / \omega_p)$ denotes the relative width of the peak with central frequency ω_p and full width at half maximum $\Delta\omega$. For $D=0.004$, the spectrum (a) represented by the dashed curve has a small peak and an SNR of 0.08. For a noise level of $D=0.015$, the spectrum (b) represented by the dotted curve shows a narrow and high first-harmonic peak, which has an SNR of 3.28. Increasing the noise to $D=0.04$ gives the spectrum (c) represented by the solid curve, which has an SNR of 0.04. Notice that the first harmonic in the spectrum for $D=0.04$ and the second harmonic for $D=0.015$ are very close together. The peak in the spectrum shifts toward higher frequencies for increasing D , because stronger noise triggers a new pulse faster; see also Fig. 8.

Notice that the amplitudes of the pulses decrease for increasing D , since increasing noise implies faster triggering and consequently less time for the gain to recover between

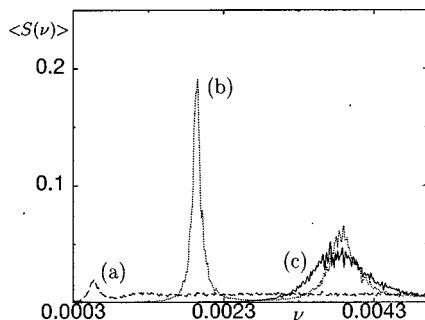


FIG. 7. Evidence of CR in the power spectra for the three different time series in Fig. 6. For $D=0.004$ (a) the SNR is 0.08, for $D=0.015 = D^R$ (b) the peak is highest and the SNR is 3.28, and for $D=0.04$ (c) the SNR is 0.28.

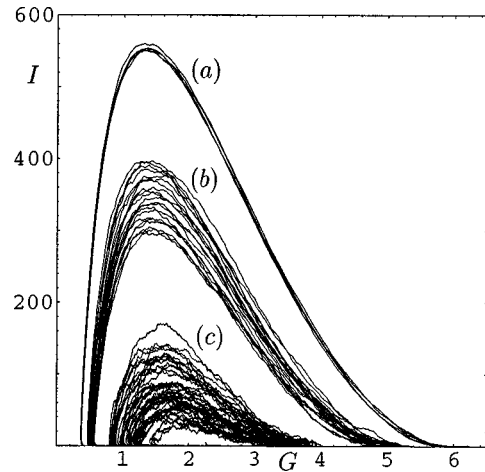


FIG. 8. Two-dimensional projection of orbits in phase space on the (G, I) plane for the three time series of Fig. 6, namely for $D = 0.004$ (a), $D = 0.015$ (b), and $D = 0.04$ (c).

two consecutive pulses. Because the gain cannot get near its unsaturated value, the amplification is reduced. This effect is clearly demonstrated in Fig. 8, where a two-dimensional projection of the trajectories on the (G, I) plane is depicted. As the noise is increased, the system is excited for smaller values of G . Notice also that the uncertainty in the (maximum) pulse amplitude and in the G value for which the system is excited increases with D ; see Figs. 6 and 8.

Another way to quantify these observations of CR is to study the pulse repetition times t_T and their fluctuations. The coherence of the pulse train is given by the normalized timing fluctuations or jitter [20],

$$R = \frac{\sigma_{t_T}}{\langle t_T \rangle}. \quad (17)$$

Here σ_{t_T} is the standard deviation of the total pulse repetition time, usually referred to as jitter in pulsating lasers. In the presence of CR, the normalized jitter R has a minimum for a particular noise level. This is indeed the case for the laser with an absorber considered here as can be seen from Fig. 9, from which the value of $D^R \approx 0.015$ can be found. We re-

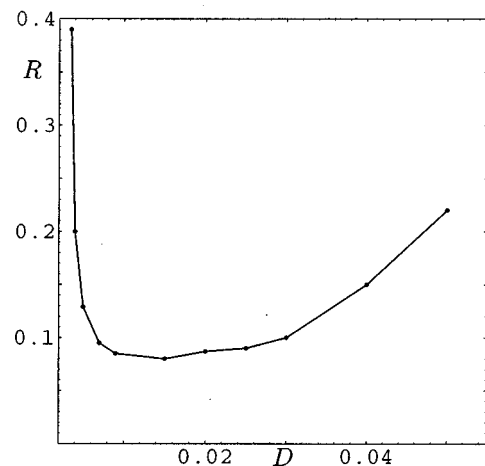


FIG. 9. The jitter R as a function of the injection noise for constant $\beta_{sp}=1.0\times 10^{-5}$.

mark that this value is close, but does not exactly coincide with the value of D for which the SNR attains its maximum, because amplitude fluctuations contribute to the SNR [28]. The evidence of CR as a function of the injected noise level D discussed above is immediately verifiable by experiment.

To explain the presence of CR in the Yamada model, we divide the pulse repetition time $t_T = t_a + t_c$ into the activation time t_a , the time needed for the noise to trigger a pulse, and the relaxation time t_c , which is the time including the pulse needed by the system to relax so that eventually a new pulse can be triggered. It is not possible to determine from the time series which part of the time t_T constitutes t_a and which part t_c ; for this one needs to consider the orbit in phase space; see Fig. 8. The different times t_a and t_c and their respective standard deviations have different dependence on the noise level. The activation time decreases with increasing noise, which is in fact a Kramers escape rate problem [24,29,30]. For low noise levels, t_a constitutes the dominant contribution to t_T and $\langle t_a^2 \rangle \approx \langle t_a \rangle^2$ [20], so that R is close to unity. When the noise is increased $\langle t_a \rangle$ decreases, as does $\langle t_a^2 \rangle$ until $\langle t_c \rangle$ constitutes the dominating contribution to $\langle t_T \rangle$ and $\langle t_c^2 \rangle > \langle t_a^2 \rangle$. The dependence of $\langle t_c \rangle$ and its fluctuations on D can be estimated by using singular perturbation theory [15], which shows that $\langle t_c \rangle$ decreases with increasing noise whereas $\langle t_c^2 \rangle$ slightly increases for sufficiently large values of D , so that R increases again. This consideration of t_a and t_c accounts for the minimum in R that constitutes CR.

The dependence of t_c and its fluctuations on the noise has the following physical explanation. When there is very little noise, each time the system gets triggered G and Q have about the same values, namely those where the excitability threshold is minimal, that is, close to the saddle point. The system is excited when the gain and the absorber relax towards their unsaturated values A and B , respectively, as in Fig. 8(a). When the noise level is increased, the system gets excited before reaching the vicinity of the saddle point. This means that the system has less time to relax, and the gain and the absorber have not recovered to their unsaturated values but remain at a certain degree of saturation as in Figs. 8(b) and 8(c). Notice the direct connection between the value of the gain and t_c : the smaller the gain at the moment of exciting a new pulse, the less gain there is for the output pulse and the shorter is t_c . However, the fluctuations in t_c do not depend so sensitively on the noise level, but are approximately constant (slightly increasing with increasing noise).

Finally we mention that injected noise also has an influence just above threshold. From previous studies of the effects of noise in lasers with a saturable absorber in the self-pulsating regime (above threshold) as performed in Refs. [23,31,12], it is known that noise has the effect of increasing the self-pulsation frequency. This shows up as a kink in the frequency versus pump current curve [23,31] and can be interpreted as the ghost of excitability: the system is kicked off the limit cycle in regime 3 of Fig. 2 by noise before it reaches the ‘‘take-off point’’ where a new pulse would begin in the absence of noise. In other words, the next pulse arises earlier than it would without noise. This constitutes an indirect experimental confirmation that the system is excitable.

V. CONCLUSIONS

We studied excitability and coherence resonance in a (semiconductor) laser with a saturable absorber as described by the Yamada model. A numerical study showed that the system can be triggered by a small input pulse to produce a single large output pulse whose shape is independent of the perturbation. The amplitude of the output pulse was demonstrated to depend linearly on the amplitude of the input pulse relative to the excitability threshold. Furthermore, we gave analytical expressions for the excitability threshold and the delay between incoming and outgoing pulses. Typical values of the spontaneous-emission factor will not influence the properties of the output pulses noticeably, so that the excitability reported here appears to be suitable for pulse reshaping.

When sufficiently strong optical noise is injected, the system shows coherence resonance. The noise results in a pulse train with minimal jitter for a particular level of injected noise. This all optical CR was explained as a direct consequence of the excitability of the system and allows experimental verification.

Practical applications of excitability and CR, for example clock recovery, pulse reshaping, and the production of tunable pulses, remain a subject for future investigations.

ACKNOWLEDGMENTS

We wish to thank J.R. Tredicce for helpful discussions. This research was supported by the Foundation for Fundamental Research on Matter (FOM), which is financially supported by the Netherlands Organization for Scientific Research (NWO).

-
- [1] J.D. Murray, *Mathematical Biology* (Springer, New York, 1990).
 - [2] S. Grill, V.S. Zykov, and S.C. Müller, *J. Phys. Chem.* **100**, 19 082 (1996).
 - [3] D. Taylor, P. Holmes, and A.H. Cohen, *Excitable Oscillators as Models for Central Pattern Generators, Series on Stability, Vibration and Control of Systems, Series B* (World Scientific Publishing Company, Singapore, 1997).
 - [4] W. Lu, D. Yu, and R.G. Harrison, *Phys. Rev. A* **58**, R809 (1998).
 - [5] J. Mullet and C.R. Mirasso, *Phys. Rev. E* **59**, 5400 (1999).
 - [6] J.L.A. Dubbeldam and B. Krauskopf, *Opt. Commun.* **159**, 325 (1999).
 - [7] G.B. Ermentrout and N. Kopell, *SIAM (Soc. Ind. Appl. Math.) J. Appl. Math.* **46**, 233 (1986).
 - [8] M. Giudici, C. Green, G. Giacomelli, U. Nespolo, and J.R. Tredicce, *Phys. Rev. E* **55**, 6414 (1997).
 - [9] G. Giacomelli, M. Giudici, S. Balle, and J.R. Tredicce (unpublished) and private communication.
 - [10] H. Gang, T. Ditzinger, C.Z. Ning, and H. Haken, *Phys. Rev. Lett.* **71**, 807 (1993).
 - [11] M. Yamada, *IEEE J. Quantum Electron.* **QE-29**, 1330 (1993).
 - [12] C.R. Mirasso, G.H.M. van Tartwijk, E.H. Garcia, D. Lenstra, P. Landais, P. Phelan, J. O’Gorgman, M. San Miguel, and W.

- Elsässer, IEEE J. Quantum Electron. **QE-35**, 764 (1999).
- [13] G.P. Agrawal and N.K. Dutta, *Semiconductor Lasers*, 2nd ed. (Van Nostrand Reinhold, New York, 1993).
- [14] R.G.M.P. Koumans and R. van Roijen, IEEE J. Quantum Electron. **QE-32**, 1122 (1994).
- [15] T. Erneux, J. Opt. Soc. Am. B **5**, 1063 (1988).
- [16] L. Gammaïtoni, P. Hänggi, P. Jing, and F. Marchesoni, Rev. Mod. Phys. **70**, 223 (1998).
- [17] J.J. Collins, C.C. Chow, and T.T. Imhoff, Phys. Rev. E **52**, R3321 (1995).
- [18] B. McNamara, K. Wiesenfeld, and R. Roy, Phys. Rev. Lett. **60**, 2626 (1988).
- [19] K. Wiesenfeld, D. Pierson, E. Pantazelou, C. Dames, and F. Moss, Phys. Rev. Lett. **72**, 2125 (1994).
- [20] A.S. Pikovsky and J. Kurths, Phys. Rev. Lett. **78**, 775 (1997).
- [21] S.G. Lee, A. Neïman, and S. Kim, Phys. Rev. E **57**, 3292 (1998).
- [22] J. Kevorkian and J.D. Cole, *Perturbation Methods in Applied Mathematics* (Springer-Verlag, New York, 1981).
- [23] M. Georgiou and T. Erneux, Phys. Rev. A **45**, 6636 (1992).
- [24] P. Hänggi, P. Talkner, and M. Borkovec, Rev. Mod. Phys. **62**, 251 (1990).
- [25] C.W. Gardiner, *Handbook of Stochastic Methods*, 2nd ed. (Springer, New York, 1997).
- [26] D. Huhse, M. Schell, W. Utz, J. Kaessner, and D. Bimberg, IEEE Photonics Technol. Lett. **7**, 351 (1995).
- [27] A. Fioretti, L. Guidoni, R. Manella, and E. Arimondo, J. Stat. Phys. **70**, 403 (1993).
- [28] D. von der Linde, Appl. Phys. B: Photophys. Laser Chem. **39**, 201 (1985).
- [29] V.I. Mel'nikov, Phys. Rep. **209**, 3 (1991).
- [30] B. Gaveau, E. Gudowska-Nowak, R. Kapral, and M. Moreau, Phys. Rev. A **46**, 825 (1992).
- [31] G.H.M. van Tartwijk and M. San Miguel, IEEE J. Quantum Electron. **QE-32**, 1191 (1996).